Nuclear Titin interacts with A- and B-type lamins in vitro and in vivo

Michael S. Zastrow[1,*], Denise B. Flaherty[2‡], Guy M. Benian[2] and Katherine L. Wilson[1,§]

[1]Department of Cell Biology, The Johns Hopkins University School of Medicine, 725 N. Wolfe St, Baltimore, MD 21205, USA
[2]Department of Pathology, Emory University, Whitehead Biomedical Research Building, Atlanta, GA 30332, USA
*Present address: Department of Developmental Biology, Stanford University School of Medicine, Beckman Center, B300, 279 Campus Drive, Stanford, CA 94305, USA
‡Department of Biology, Eckerd College, SHB 105, 4200 54th Ave, St Petersburg, FL 33711, USA
§Author for correspondence (e-mail: klwilson@jhmi.edu)

Accepted 4 October 2005
Journal of Cell Science 119, 239-249 Published by The Company of Biologists 2006
doi:10.1242/jcs.02728

Summary

Lamins form structural filaments in the nucleus. Mutations in A-type lamins cause muscular dystrophy, cardiomyopathy and other diseases, including progeroid syndromes. To identify new binding partners for lamin A, we carried out a two-hybrid screen with a human skeletal-muscle cDNA library, using the Ig-fold domain of lamin A as bait. The C-terminal region of titin was recovered twice. Previous investigators showed that nuclear isoforms of titin are essential for chromosome condensation during mitosis. Our titin fragment, which includes two regions unique to titin (M-is6 and M-is7), bound directly to both A- and B-type lamins in vitro. Titin binding to disease-causing lamin A mutants R527P and R482Q was reduced 50%. Studies in living cells suggested lamin-titin interactions were physiologically relevant. In *Caenorhabditis elegans* embryos, two independent *C. elegans* (Ce)-titin antibodies colocalized with Ce-lamin at the nuclear envelope. In lamin-downregulated [lmn-1(RNAi)] embryos, Ce-titin was undetectable at the nuclear envelope suggesting its localization or stability requires Ce-lamin. In human cells (HeLa), antibodies against the titin-specific domain M-is6 gave both diffuse and punctate intranuclear staining by indirect immunofluorescence, and recognized at least three bands larger than 1 MDa in immunoblots of isolated HeLa nuclei. In HeLa cells that transiently overexpressed a lamin-binding fragment of titin, nuclei became grossly misshapen and herniated at sites lacking lamin B. We conclude that the C-terminus of nuclear titin binds lamins in vivo and might contribute to nuclear organization during interphase.

Key words: Titin, Nuclear envelope, Lamin A, Laminopathy, Emery-Dreifuss muscular dystrophy

Introduction

Lamins are type-V intermediate filament proteins essential for the architecture of metazoan nuclei (Goldman et al., 2002). Lamins have three domains: a small N-terminal globular head, a long coiled-coil rod and a large C-terminal globular tail. Lamins exist as coiled-coil dimers, which polymerize head-to-tail. These polymers then associate laterally to form filaments (Stuurman et al., 1998). In *Xenopus laevis* oocyte nuclei, lamins form orthogonal networks of filaments about 10-nm in diameter, as visualized by electron microscopy (Aebi et al., 1986). Although lamin filaments concentrate near the nuclear inner membrane ('peripheral' lamina), lamins also localize inside the nucleus ('interior' lamina) (Moir et al., 2000a). Lamins provide structural and mechanical support for the nucleus (Dahl et al., 2004; Lammerding et al., 2004), determine nuclear shape and anchor nuclear pore complexes (Gruenbaum et al., 2003). Lamins also support fundamental activities including mRNA transcription and DNA replication (Moir et al., 2000b; Spann et al., 2002). To explain this lamin-dependence, many different proteins and oligomeric complexes are proposed to use lamins as scaffolds for their own assembly or function (Gruenbaum et al., 2005; Zastrow et al., 2004).

Mammals express both A- and B-type lamins. The *Lmna* gene gives rise to four alternatively-spliced A-type lamins: A, C, AΔ10 and C2 (Lin and Worman, 1993). The lamin A precursor (pre-lamin A) is posttranslationally processed to generate mature lamin A. *Lmnb1* and *Lmnb2* encode lamin B1 and lamins B2/B3, respectively (Lin and Worman, 1995). Downregulation studies using small interference RNA (siRNA) in mammalian cells (Harborth et al., 2001) and *C. elegans* (Liu et al., 2000) showed that B-type lamins are essential. By contrast, A-type lamins are not essential for cell viability, but *Lmna*-knockout mice develop muscular dystrophy and die within eight weeks after birth (Sullivan et al., 1999). A-type lamins are developmentally regulated and highly expressed in most differentiated cells, suggesting tissue-specific functions. Interestingly, A- and B-type lamins appear to form independent filament networks in vivo (Izumi et al., 2000; Steen and Collas, 2001).

In humans, dominant mutations in *LMNA* cause at least ten diseases, termed 'laminopathies', which affect specific tissues. One such disease is Emery-Dreifuss muscular dystrophy (EDMD), characterized by muscle wasting, contractures of major tendons and cardiac conduction system defects that can cause sudden cardiac arrest (Bonne et al., 1999). Other laminopathies selectively affect skeletal muscle (limb-girdle muscular dystrophy 1B; LGMD1B), heart (dilated cardiomyopathy 1A; DCM1A) or neurons, or a combination of tissues. For example, Charcot-Marie-Tooth disease (CMT) (De Sandre-Giovannoli et al., 2002) affects neurons, whereas

mandibuloacral dysplasia (MAD) (Novelli et al., 2002) and familial partial lipodystrophy (FPLD, Dunnigan type) (Shackleton et al., 2000) both cause lipodystrophy and diabetes. Severe laminopathies can be lethal (restrictive dermatitis) (Navarro et al., 2004) or cause accelerated 'aging' syndromes such as Hutchinson-Gilford progeria syndrome (HGPS) (De Sandre-Giovannoli et al., 2003; Eriksson et al., 2003) and atypical Werner Syndrome (Chen et al., 2003). Children with HGPS experience growth retardation, hair loss, skin-aging and -wrinkling, loss of white-fat tissue, progressive heart disease and death in the early teens from stroke or cardiovascular disease (Mounkes and Stewart, 2004; Ostlund and Worman, 2003).

At least 16 different binding partners for A-type lamins have been identified so far (reviewed by Zastrow et al., 2004). Several partners, including the transcription repressor Rb (Mancini et al., 1994), are involved in signaling or gene regulation. However, other partners have potential architectural roles including actin (Pederson and Aebi, 2002; Sasseville and Langelier, 1998) and the nesprin family of spectrin-repeat proteins (Mislow et al., 2002a; Mislow et al., 2002b; Padmakumar et al., 2004; Zhang et al., 2002; Zhang et al., 2001). Interestingly, mammalian cells that lack A-type lamins are both mechanically weak and defective in mechanically-regulated gene expression (Lammerding et al., 2004).

Given the variety of disease phenotypes caused by mutations in *LMNA*, we hypothesized that lamin A might have additional partners preferentially expressed in disease-affected tissues, such as muscle. To test this hypothesis, we used a yeast two-hybrid assay to screen a human skeletal-muscle cDNA library for proteins that bind the Ig-fold domain in the tail of lamin A. Here, we report the results of this screen, which yielded an unanticipated structural partner: nuclear titin. Approximately one third of the 363 exons of the human titin gene *TTN* are alternatively-spliced, yielding numerous titin isoforms up to 3 MDa in mass (Granzier and Labeit, 2004; Tskhovrebova and Trinick, 2003). Cytoplasmic isoforms of titin have familiar roles in the organization and elastic properties of muscle sarcomeres (Tskhovrebova and Trinick, 2003). However, in non-muscle cells, nuclear isoform(s) of titin are essential for chromosome condensation and chromosome segregation during mitosis, as shown in *Drosophila melanogaster* embryos (Machado and Andrew, 2000; Machado et al., 1998). We show that the interphase localization of titin depends on lamins in *C. elegans,* and lamin-binding fragments of titin – when overexpressed in mammalian cells – disrupt nuclear lamina integrity and nuclear architecture.

Results

The bait for our yeast two-hybrid screen was the polypeptide encoded by exons 8-9 in the tail domain of human *LMNA* (Fig. 1A). Subsequent work revealed that this polypeptide (residues 461-536) comprises most of a lamin-specific Ig-fold domain (Dhe-Paganon et al., 2002; Krimm et al., 2002). This bait was negative for auto-activation of reporter genes (data not shown) and was used to screen 2×10^7 clones, providing an over fivefold coverage of the 3.5×10^6 independent clones represented in the pre-transformed human skeletal muscle cDNA library (see Materials and Methods). Our screen yielded 185 triple-selection-positive clones (growth on plates lacking Trp, Leu and His), 42 of which encoded actin. Of the remaining

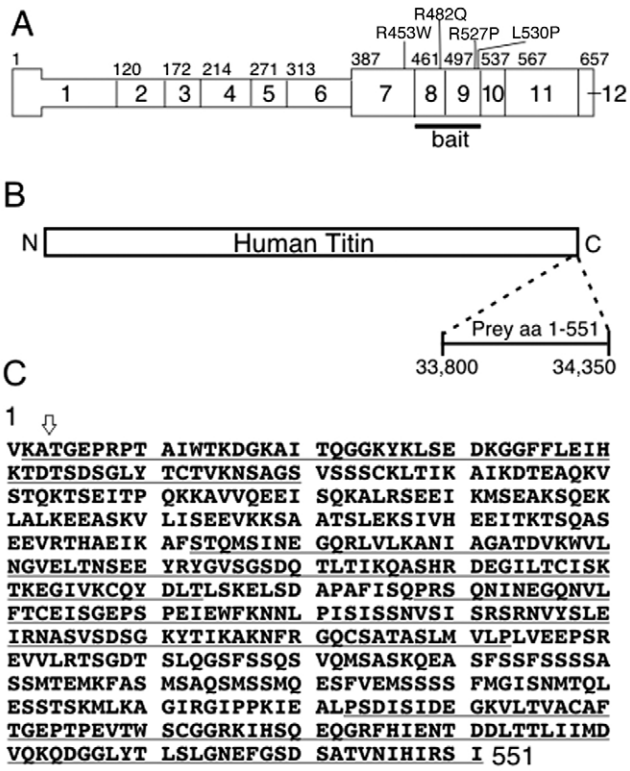

Fig. 1. Two-hybrid bait and titin polypeptides identified in the two-hybrid screen. (A) Diagram of the pre-lamin A protein drawn to scale, showing regions encoded by exons 1-12. The exon 8-9 bait polypeptide is underlined (bait). Vertical lines indicate positions of missense mutations that cause EDMD (R527P, R453W), MAD (L530P) or FPLD (R482Q). (B) Schematic drawing of the human titin protein (NP_596869; 34,350 residues) showing the position of the lamin-binding fragment (prey). (C) Amino acid sequence of the lamin-binding region of human titin. The arrow indicates the first residue encoded by the smaller two-hybrid titin isolate. The larger isolate encodes a 61 kDa polypeptide termed titin 1-551. Four predicted Ig-fold domains are underlined. Non-underlined regions correspond to titin-specific regions M-is6 (residues 61-172) and M-is7 (residues 353-462).

143 actin-negative clones, 35 (including a representative actin isolate) survived quadruple-selection (plates lacked Trp, Leu, His and Ade) and also expressed the third two-hybrid-dependent gene, β-galactosidase (data not shown).

The 35 true-positive clones were each transformed into yeast that either contained a freshly transformed bait plasmid or not, and tested under quadruple selection in the presence of X-Gal. All 35 cDNAs conferred survival with varying levels of β-galactosidase activity in the presence of the lamin bait; all 35 failed to survive in cells that lacked the lamin bait, suggesting they were bona fide two-hybrid-selection-positive clones (data not shown). DNA sequence analysis identified these cDNAs and showed that the majority (19 out of 35) were recovered only once in the screen; these were not pursued and their significance remains unknown. Polypeptides representing the C-terminus of human titin (Fig. 1B) were independently isolated twice – with substantial overlap: the encoded polypeptides differed by only three residues (Fig. 1C, arrow indicates first residue of shorter isolate).

Full-length human titin has multiple Ig-fold and fibronectin-type-3 domains (~166 and ~132 copies, respectively), and one PEVK domain (Amodeo et al., 2001; Linke et al., 2002). The larger titin cDNA recovered in our screen encoded the C-terminal 551 residues of human titin (GenBank accession number NP_596869; Fig. 1B,C), hereafter designated titin 1-551. In the sarcomere, titin 1-551 localizes to the M-line region. The titin 1-551 polypeptide has four predicted Ig-fold domains (named M7 to M10) and two titin-specific domains that are not found in other proteins (named M-is6 and M-is7, residues 61-172 and 353-462, respectively) [Fig. 1C; for nomenclature see Labeit and Kolmerer (Labeit and Kolmerer, 1995)]. Interestingly, a mutation in the Ig-fold M10 of titin causes tibial muscular dystrophy (Hackman et al., 2003).

Biochemical confirmation of the lamin-titin interaction

Lamin binding to titin 1-551 was verified in several independent biochemical assays. Bacterially expressed and purified pre-lamin A tail residues 394-664, His-tagged at the C-terminus, were coupled to Ni^{2+}-NTA-agarose beads and incubated with ^{35}S-titin 1-551 (see Materials and Methods). As the negative control, lamins were omitted. Bound proteins were extracted with SDS sample buffer, resolved by SDS-PAGE and detected by autoradiography (Fig. 2A). ^{35}S-Titin 1-551 bound efficiently to the lamin-beads, but not to control beads, biochemically confirming the two-hybrid interaction. A second ('microtiter') assay, in which purified pre-lamin A tails (or BSA) were immobilized in microtiter wells and incubated with increasing amounts of ^{35}S-titin 1-551, independently confirmed the interaction (Fig. 2B).

To determine whether titin also recognized B-type lamins, we used a third assay in which His-tagged pre-lamin A tail or lamin B1 tail (residues 395-586) were conjugated to AffiGel beads. BSA-conjugated beads served as negative controls. Beads were incubated with ^{35}S-titin 1-551, and the bound (pelleted, P) versus unbound (supernatant, S) titin was resolved by SDS-PAGE and visualized by autoradiography (Fig. 2C; upper panel). Binding was quantified by densitometry (Fig. 2D) relative to each input His-tagged lamin (Fig. 2C; lower panel). Titin 1-551 bound both A- and B-type lamin tails significantly above the BSA controls, with a slight (1.3-fold) preference for lamin A (Fig. 2D). We concluded that titin recognizes conserved residues in the Ig-fold domain of A- and B-type lamins, and that its affinity might be increased by lamin A-specific residues. Interestingly, many disease-causing mutations in lamin A alter residues that are identical or conserved between A- and B-type lamins (Cohen et al., 2001). We, therefore, tested the effects of four disease-causing missense mutations on titin binding; in each case, the native residue is exposed on the surface of the Ig-fold domain (Dhe-Paganon et al., 2002; Krimm et al., 2002). ^{35}S-titin 1-551 binding to the lamin A tail was reduced ~50% by mutations R527P (which causes EDMD) and R482Q (which causes FPLD; Fig. 2C,D). Residues R527 and R482 are both located on one side of the lamin Ig-fold domain. By contrast, the R453W mutation had no detectable affect, and the L530P mutation reduced binding only slightly (borderline statistical significance; Fig. 2C,D); these residues are located on the opposite side of the Ig-fold. Thus titin appeared mildly but selectively sensitive to disease-causing missense mutations in the Ig-fold domain of lamin A. Titin 1-551 bound normally to pre-lamin A tails bearing the 50-residue deletion that causes HGPS (Fig. 2C,D; 'Prog'); this deletion lies outside the Ig-fold domain. These results implicate the R527- and R482-containing face of the Ig-fold in binding to titin.

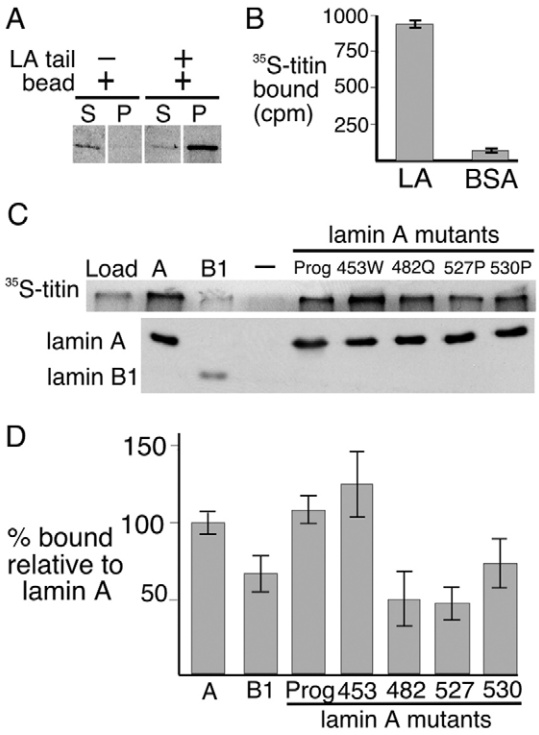

Fig. 2. Biochemical confirmation of lamin-titin binding using three independent assays. (A) Titin and lamins interact in Ni^{2+} pull-down assays. ^{35}S-titin 1-551 was incubated with His-tagged wild-type pre-lamin A tail, and pelleted with Ni^{2+}-NTA agarose beads; 20% of each supernatant and 50% of each pellet were resolved by SDS-PAGE (12% gels) and exposed to X-ray film (autoradiograph is shown). (B) Results of the microtiter-well binding assays, in which either the purified pre-lamin A tail or BSA were immobilized in microtiter wells and incubated with 1 nM ^{35}S-titin 1-551 (see Materials and Methods). The data are representative of five independent experiments, each done in triplicate. (C) Binding to lamin-AffiGel beads. Purified recombinant pre-lamin A tail (wild type or mutants; 'prog' indicates pre-lamin A with the 50-residue deletion that causes HGPS) or lamin B1 tail were coupled covalently to AffiGel beads, incubated with ^{35}S-titin 1-551 and pelleted to recover bound probe. Pellets (50% of each sample) were resolved by SDS-PAGE and autoradiographed (^{35}S-titin; upper panel) or immunoblotted with antibodies against the His-tag on each lamin tail (lower panel). (D) Quantification of data from panel C plotted as % of each probe that bound and normalized against titin binding to wild-type pre-lamin A tail. Bars indicate standard deviations from four independent experiments.

Lamin-binding regions in titin 1-551

To determine which domain(s) in titin 1-551 were sufficient to bind lamin A, we synthesized full-length ^{35}S-titin 1-551 (Fig. 3A, fragment 6) and five subfragments designated fragment 1 (residues 1-172), fragment 2 (residues 61-172), fragment 3 (residues 173-352), fragment 4 (residues 353-462) and fragment 5 (residues 353-551; Fig. 3A). Each subfragment was tested for binding to pre-lamin A tails in solution. We coupled

the bacterially-expressed purified His-tagged pre-lamin A tail to Ni^{2+}-agarose beads, then incubated with each ^{35}S-titin fragment, washed and pelleted the beads (Fig. 3B), and used densitometry to quantify the ratio of bound (pelleted, P) to unbound (supernatant, S) probe (Fig. 3C; 20% of each sample loaded). These experiments showed optimal binding by full-length fragment 6, consistent with our two-hybrid results. Fragment 2 did not detectably bind to the pre-lamin tail (Fig. 3C). Fragments 1, 3 and 4 each bound lamin independently, with approximately equal efficiencies (35-50% of each probe bound; Fig. 3C). Fragment 5, comprising M-is7 and M-10, bound almost twice as well as M-is7 alone and ~65% as well as full-length fragment 6. Comparing fragments 4 and 5, we deduced that M10 also has affinity for lamin. Fragment 6 (full-length) bound over threefold more efficiently than any single domain alone. We, therefore, concluded that the titin 1-551 polypeptide contains at least four domains (M7, M8/9, M-is7 and M10) that, individually, are capable of binding lamin, all contributing to titin's affinity for lamin A.

Antibodies against the M-is6 domain of human titin stain HeLa cell nuclei

Titin is detectable by indirect immunofluorescence in the nuclei of human Hep2 cells (Machado et al., 1998). To find out whether titin isoforms that contain the titin 1-551 polypeptide localized in the nucleus, we generated rabbit polyclonal serum 5460 against the M-is6 domain. We hoped that this domain, which did not bind lamin A, would be accessible to antibodies in vivo. Immunoblot analysis of lysates from HeLa cells transiently transfected with cDNAs encoding green fluorescent protein (GFP) and a nuclear localization sequence fused to M-is6 (GFP-is6), revealed one major band of ~37 kDa – the predicted mass of GFP-is6. This band was not detected by pre-immune serum (Fig. 4A, PI) and was competed by purified M-is6 protein (Fig. 4A, Inh). To determine whether serum 5460 also detected endogenous titin, we resolved untransfected HeLa cell lysates and extracts from isolated HeLa nuclei, using titin-compatible conditions on SDS-PAGE gels with a 2.5-7.5% gradient, and probed with either immune serum 5460 (Fig. 4B, Im), serum 5460 pretreated with purified M-is6 antigen (Fig. 4B, Inh), or pre-immune serum 5460 (Fig. 4B, PI). The 5460 antibodies recognized one major band at the top of the gel (significantly greater than 1 MDa) in both whole cell lysates (Fig. 4B, cells) and isolated nuclei (Fig. 4B, nuclei). Isolated nuclei contained two additional bands with a mass of more than 600 kDa, which were either breakdown products or nuclear-enriched isoforms of titin. Recognition of these enormous proteins was significantly reduced by competition with purified antigen, and none were recognized by pre-immune serum (Fig. 4B, PI). This strongly suggests that our antibody against the M-is6 domain specifically recognized endogenous cellular and nuclear titin. We concluded that at least one titin isoform containing the M-is6 domain exists in the nuclei of non-muscle (HeLa) cells, consistent with potential in-vivo interaction with lamins.

Indirect immunofluorescent staining of untransfected HeLa cells with serum 5460 revealed punctate and diffuse staining of the nucleus and, to a lesser extent, the cytoplasm (Fig. 4C, 5460 Im). These signals were blocked by pretreatment with purified M-is6 polypeptide (Fig. 4C; Im + Ag) and absent from pre-immune controls (Fig. 4C, PI), suggesting specific recognition. Diffuse and punctate intranuclear staining was also seen in nuclei isolated from untransfected HeLa cells, and these signals were significantly higher than the pre-immune and antigen-pretreated controls (Fig. 4D, Im+Ag and PI, respectively). We concluded that the M-is6 domain of endogenous titin localizes throughout the nucleus. Interestingly, a subset of titin-positive puncta potentially colocalized with lamin A (Fig. 4D, arrows), consistent with potential interactions in vivo. We concluded that the lamin-binding region of endogenous human titin localizes in the nucleus.

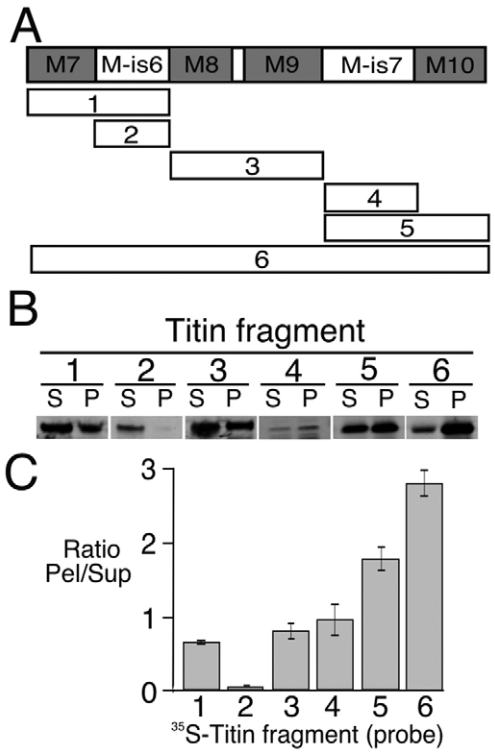

Fig. 3. Mapping the lamin-binding regions in titin 1-551. (A) Schematic diagram of titin 1-551, showing locations of predicted Ig-fold domains (gray) and titin-specific domains M-is6 and M-is7. Bars numbered 1-6 represent the titin subfragments tested for binding to the pre-lamin A tail. (B) Autoradiograph showing ^{35}S-labeled titin fragments bound to His-tagged pre-lamin A tail (on Ni^{2+} beads). Corresponding unbound (supernatant, S) and bound (pellet, P) fractions (20% each) were resolved by SDS-PAGE and exposed to film. (C) Data from panel B are shown as the ratio of bound:unbound probe for ^{35}S-titin fragments 1-6. Bars indicate standard deviations from four independent experiments.

Expression of titin fragment M-is7 in HeLa cells disrupts lamin B and produces misshapen, herniated nuclei

The above two-hybrid results and also three independent direct-binding assays collectively showed that the C-terminal region of human titin binds lamins in vitro. The nuclear localization of titin further suggested that titin interacts with lamins in cells. To determine whether this binding is physiologically relevant, we transiently transfected HeLa cells with a cDNA encoding GFP-NLS fused to M-is7 (GFP-is7), the titin-specific domain that binds lamin A (Fig. 3). Negative-control cells were either untransfected (Fig. 5A, Un) or

transfected with GFP-NLS fused to pyruvate kinase (GFP-PK; Fig. 5A, PK) or M-is6 (GFP-is6), which does not bind lamins (Fig. 5B, +is6). Of the cells that expressed GFP-is7, 41% had deformed nuclei (n=250 transfected cells; Fig. 5A,C), compared to only 5.6% of untransfected cells (n=250), 9.6% of cells expressing GFP-PK (n=250) and 6.4% of cells expressing GFP-is6 (n=250; Fig. 5C). Control cells stained by indirect immunofluorescence showed a continuous nuclear envelope 'rim' signal for lamin B and, as expected, diffuse intranuclear staining (Fig. 5A,B; lamin B). However, cells that expressed GFP-is7 had large gaps in the staining of lamin B at the nuclear envelope (Fig. 5A; + is7, white arrowheads in lamin B images). These gaps corresponded to nuclear envelope herniations, which were filled with GFP-is7 and devoid of both lamin B and chromatin (Fig. 5A; white arrowheads in merged images). We concluded that the overexpressed M-is7 polypeptide bound lamins in vivo and competed for sites needed by other lamin-binding proteins (possibly including endogenous titin) to maintain nuclear architecture.

To directly test for in-vivo binding between M-is7 and lamins, we immunoprecipitated GFP-is7-transfected HeLa cells with antibodies against GFP using protein-A-coupled magnetic beads. Samples were resolved by SDS-PAGE and immunoblotted with a mixture of antibodies against A-type lamins and lamin B1 (Fig. 5D). Lamins remained in the supernatant when antibodies against GFP were omitted (Fig. 5D, GFP –). However, A-type lamins and, to a lesser extent, lamin B1 (possibly due to different solubility of A- and B-type lamins) bound specifically to the M-is7 beads (Fig. 5D). This result was consistent with our in-vitro pull-down experiments (Fig. 2), where M-is7 bound both types but favored A over B. Interestingly, M-is7 also bound lamin C, the other abundant A-type lamin. Thus, we concluded that human titin binds both A- and B-type lamins in vivo.

Titin colocalizes with lamins at the nuclear envelope in *C. elegans* embryos

To independently determine whether titin-lamin interactions are biologically relevant, we tested the hypothesis that the nuclear localization of titin depends on lamins. For simplicity, we did this experiment in the nematode *C. elegans*, which encodes a single B-type lamin (*lmn-1*) (Liu et al., 2000), *C. elegans* (Ce)-titin and three titin-related proteins named twitchin, UNC-89 and Ce-kettin, encoded by *unc-22*, *unc-89* and *ketn-1,* respectively (Flaherty et al., 2002).

We first localized endogenous Ce-titin with three independent antibodies raised against recombinant polypeptides from the N-terminus (EU145 region), middle (EU102 region) and C-terminus (EU143

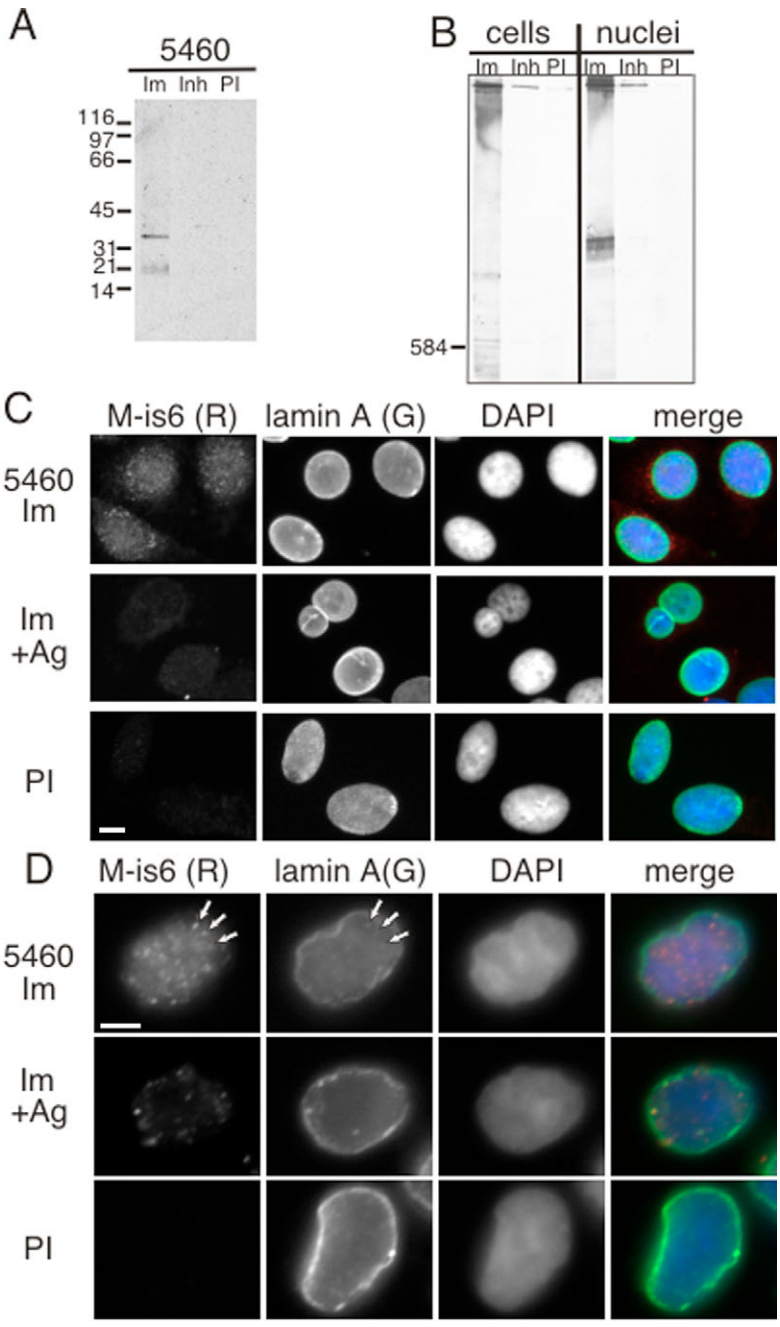

Fig. 4. Localization of M-is6 epitopes in HeLa cells. (A) Immunoblot analysis of lysates from HeLa cells transfected with GFP-is6 and probed with immune rabbit serum 5460 against M-is6 (5460; Im), preimmune serum 5460 (PI), or immune 5460 pretreated with purified M-is6 protein (Inh). (B) Immunoblots of protein lysates of whole HeLa cells (cells) or purified HeLa nuclei (nuclei) separated on 2.5-7.5% SDS-PAGE to resolve high molecular-weight proteins. Strips were probed using serum 5460 as in (A). The 584-kDA molecular mass marker consisted of crosslinked phosphorylase B (Sigma, St Louis, MO). (C) Indirect immunofluorescence localization of endogenous titin M-is6 epitopes in HeLa cells. Cells were triple-stained with immune rabbit serum 5460 against M-is6 (red, Cy3), or serum 5460 preincubated with purified M-is6 antigen (Im + Ag), or pre-immune serum 5460 (PI) and counter-stained using antibodies against lamin A (green; FITC) and DAPI to stain DNA. (D) Indirect immunofluorescence staining of isolated HeLa cell nuclei using the same antibodies as in (A). Arrows indicate three of many puncta in which lamin A and titin potentially colocalized. Bars, 2 μm.

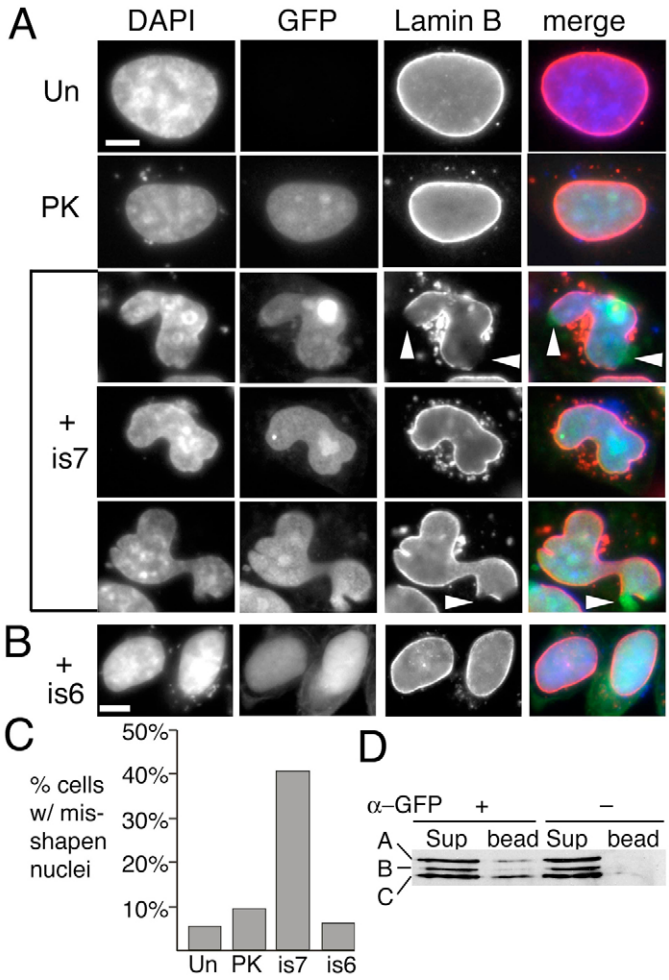

Fig. 5. Phenotype of HeLa cells transiently overexpressing GFP-fused M-is7, PK or M-is6. HeLa cells were examined 24 hours after transfection by fixing and staining with antibodies specific against lamin B (red, Cy3), staining with DAPI for DNA (blue) and visualizing GFP fluorescence (green). Untransfected cells (Un) were included as controls. Cells expressing GFP-is7 had a high frequency of aberrantly-shaped nuclei and nuclear envelope herniations (arrowheads) that contained GFP-is7, but not chromatin or lamin B. (B) HeLa cells overexpressing GFP-is6, which does not bind lamins in vitro, have normal nuclear shape and lamin organization. Bars, 2 μm. (C) Percentage of cells with deformed nuclei; *n*=250 cells per group. (D) Lysates from HeLa cells overexpressing GFP-is7 were immunoprecipitated with antibodies against GFP, or no antibody as a control; lanes contain supernatant (Sup, 10% of sample) and magnetic-bead-associated pellet (bead, 20% of sample). Fractions were resolved by SDS-PAGE and probed with a mixture of antibodies NC-5 and NC-7 against lamins A/C and B1, respectively.

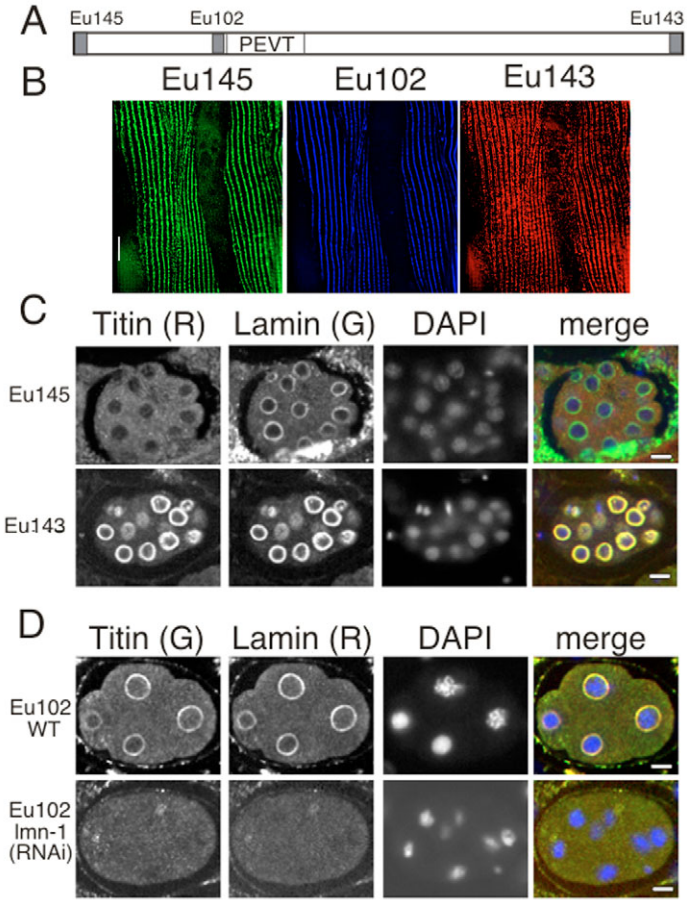

Fig. 6. (A) Schematic diagram of *C. elegans* titin protein (Ce-titin) showing the PEVT domain and polypeptide antigens used to raise antibodies EU145, EU102 and EU143 (grey boxes). (B) Adult *C. elegans* stained by indirect immunofluorescence for endogenous Ce-titin using affinity-purified EU102, EU145 and EU143 antibodies. All three gave typical striated staining in the muscle myofilament lattice. (C) Indirect immunofluorescence staining for endogenous Ce-titin (R, red; Cy3) and Ce-lamin (G, green; FITC) in wild-type embryos stained with affinity-purified EU145 or EU143 antibodies. DNA was stained with DAPI. Ce-lamin was detected with rabbit serum 3932 (Gruenbaum et al., 2002). (D) Indirect immunofluorescence staining for endogenous Ce-titin using rabbit polyclonal EU102 (G, green; FITC) and Ce-lamin rat serum 3933 (R, red; Cy3). DNA was stained with DAPI in wild-type (WT) or lmn-1(RNAi) embryos. Bars, 5 μm.

region) of a predicted 2.2 MDa Ce-titin isoform (Fig. 6A) (Flaherty et al., 2002). Indirect immunofluorescence staining of adult *C. elegans* with the anti-EU102, anti-EU143 and anti-EU145 antibodies confirmed a characteristic striated titin signal in muscle cells (Fig. 6B). To localize Ce-titin in non-muscle cells, we used confocal microscopy to visualize embryos single-labeled by indirect immunofluorescence with anti-EU102 antibody. These antibodies stained the nuclear envelope (see Fig. 7, INT and PRO), consistent with a hypothesised interaction with Ce-lamin. To test this possibility, we used confocal microscopy to visualize embryos double-labeled for endogenous Ce-lamin (Fig. 6C,D) plus antibodies against each region of Ce-titin. Antibodies anti-EU143 (Fig. 6C) and anti-EU102 (Fig. 6D) both colocalized with Ce-lamin at the nuclear envelope. By contrast, antibodies against the N-terminal (EU145) epitope did not recognize the nuclear envelope (Fig. 6C, top) above the background seen in control embryos that lack the primary or secondary antibody (not shown). The anti-EU145 antibody provided an additional control to show that the nuclear-envelope signals for antibodies anti-EU102 and anti-EU143 are not due to bleed-through lamin signals. We concluded that the middle and C-terminal

regions of Ce-titin each colocalize with near Ce-lamin at the nuclear envelope.

The nuclear-envelope localization of Ce-titin depends on lamin B

Except for matefin (Fridkin et al., 2004), all tested lamin-binding proteins in *C. elegans* are mislocalized in lamin-depleted cells (Gruenbaum et al., 2002; Liu et al., 2000; Liu et al., 2003). To determine whether the nuclear envelope localization of Ce-titin depends on Ce-lamin, we used a previously established RNAi-feeding protocol to downregulate *lmn-1* (Liu et al., 2000), and then stained embryos by double immunofluorescence for endogenous Ce-lamin and Ce-titin. In control *C. elegans* embryos, from adults fed untransformed bacteria, the anti-EU102 antibody colocalized with Ce-lamin at the nuclear envelope (Fig. 6D, WT) as expected. However, lmn-1(RNAi) embryos, which had undetectable Ce-lamin staining, also had significantly reduced Ce-titin signals at the nuclear envelope [Fig. 6D, lmn-1(RNAi)]. We concluded that, in interphase nuclei, either the stability of Ce-titin or the nuclear-envelope localization of Ce-titin depends on Ce-lamins.

Since titin has previously been linked to mitotic chromosome condensation in *Drosophila* (Machado and Andrew, 2000), we localized the endogenous Ce-titin EU102 epitope by indirect immunofluorescence staining in embryos fixed at different stages of mitosis. The Ce-titin epitope(s) localized at the nuclear envelope through prophase, then shifted to centrosomes and mitotic spindles during prometaphase, and coalesced around centrosomes during metaphase and early anaphase (Fig. 7). Ce-titin staining was diffuse in late anaphase, when nuclear envelope breakdown is complete in *C. elegans*, and Ce-lamin is entirely dispersed into the cytoplasm (Lee et al., 2000). Ce-titin then accumulated again at the nuclear envelope during telophase, when the nuclear envelope reassembles. Thus, the titin epitope was either masked or dispersed (not degraded) during late anaphase. The anti-EU143 antibody was not tested. We concluded that the EU102 epitope of Ce-titin changes location dynamically during the cell cycle: it moves from the nuclear envelope and/or lamina to the centrosome and/or mitotic spindle during mitosis, and later re-accumulates at the newly-assembled nuclear envelope.

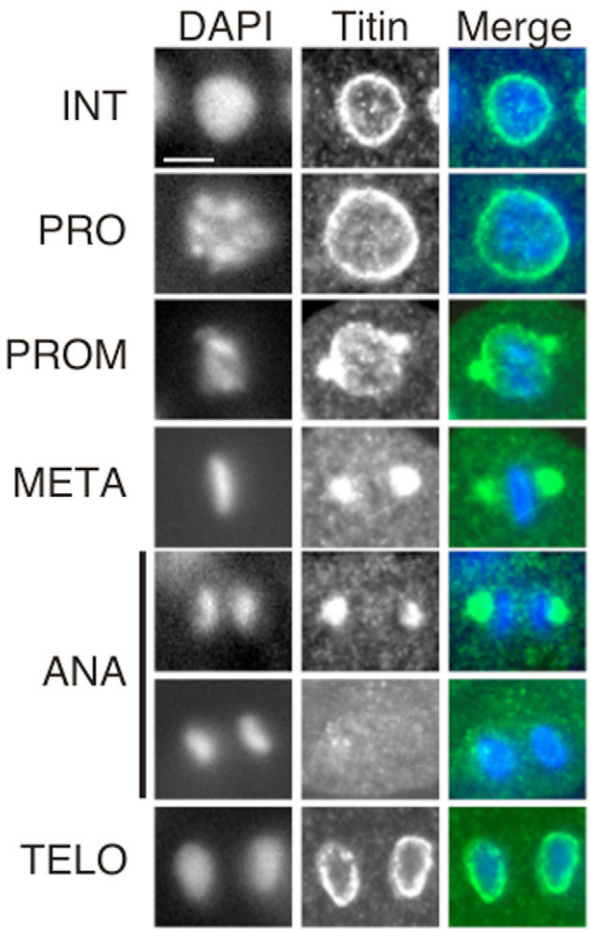

Fig. 7. Cell-cycle-dependent localization of endogenous Ce-titin in *C. elegans* embryos stained with antibody EY102 against Ce–titin (green, FITC) and DAPI to visualize DNA (blue). Stages of mitosis were inferred from chromosome morphology: interphase (INT), prophase (PRO), pro metaphase (PROM), metaphase (META), early and late anaphase (ANA), and telophase (TELO). Bar, 5 μm.

Discussion

This work shows that the C-terminal 551 residues of human titin bind both A- and B-type lamins in vitro and in vivo. Multiple subregions of titin (Ig-folds M7 to M10, and M-is7) contributed independently to lamin binding in vitro. Lamins might also bind other regions in titin not recovered in our screen. In *C. elegans*, the nuclear-envelope localization (or epitope accessibility) of Ce-titin depends on lamin B. The conserved recognition of B-type lamins and the lamin-dependent nuclear envelope localization of Ce-titin suggest that lamin-titin interactions are conserved in metazoan evolution. This interaction might be important for nuclear architecture, because HeLa cells that overexpress the M-is7 domain of titin have deformed nuclei and gaps in their lamin B network. We deduce that, the overexpressed M-is7 polypeptide competitively inhibits endogenous titin and potentially also competes with other architectural proteins that bind this same region (Ig-fold domain) in the lamin tail (candidates include actin, emerin and LAP2α) (see Zastrow et al., 2004). However, DNA also binds this region, as do signaling proteins 12(S)-lipoxygenase and sterol response element binding protein 1 (SREBP1) (Zastrow et al., 2004), so the overexpressed titin fragment probably has pleiotropic effects. Nevertheless, the dramatic changes in nuclear shape and loss of spherical integrity strongly suggest that the M-is7 region of nuclear titin binds lamins in vivo, an idea further supported by the co-immunoprecipitation of M-is7 with endogenous lamins from transfected HeLa cells. Isolated HeLa nuclei contain at least one – and perhaps three – major titin isoforms with masses in the MDa range. Thus, future challenges are to characterize nuclear-specific titin(s) to understand what features distinguish them from sarcomeric titins and each other.

Loss of *Drosophila* titin is lethal during mitosis. In *Drosophila* embryos homozygous for a deletion in D-titin, chromosomes fail to condense properly during prophase, have defective sister chromatin cohesion and missegregate during mitosis (Machado and Andrew, 2000). At least two D-titin

epitopes localize exclusively on chromosomes during mitosis in *Drosophila* embryos (Machado et al., 1998). By contrast, the Ce-titin epitope (EU102) tested in *C. elegans* did not localize to chromosomes during mitosis. Instead, it moved to the mitotic spindle and/or centrosomes and was then either transiently dispersed or masked. Why did our Ce-titin antibodies not stain chromatin, as seen for D-titin? The most likely explanation is that our antibodies recognize different epitopes on a potentially non-orthologous protein in a different species. As noted above, Ce-titin is one of at least four titin-like proteins encoded by *C. elegans*: Ce-titin (Flaherty et al., 2002), UNC-89 (Small et al., 2004), Ce-kettin (Hakeda et al., 2000) and twitchin (UNC-22) (Benian et al., 1996a). It remains unclear which *C. elegans* gene is functionally orthologous to D-titin. Moreover, even if Ce-titin and D-titin were orthologous, their splicing patterns in embryos (our *C. elegans* studies) and larvae (the *Drosophila* studies) (Machado and Andrew, 2000) might differ. Finally, one mammalian titin molecule can span 1.2 μm (Tskhovrebova and Trinick, 2003), thus the two epitopes localized in our study do not rule out the existence of chromatin-associated epitopes in other regions of the molecule.

Mutations in titin cause muscle disorders, including hypertrophic cardiomyopathy, autosomal dominant dilated cardiomyopathy and tibial muscular dystrophy (Hackman et al., 2003). Thus, mutations in either *LMNA* or *TTN* can lead to dilated cardiomyopathy or muscular dystrophy. Defects in titin are very likely to directly weaken sarcomere organization in muscle cells. Our findings raise the additional possibility that nuclear architecture might also be compromised in titin mutants. Interestingly, the kinase domain of sarcomere-localized titin regulates muscle-gene expression through mechanical load-stimulated activation of the serum response transcription factor SRF (Lange et al., 2005). We speculate that nuclear titin senses mechanical load in the nuclei of non-muscle cells.

The spatial organization of titin in interphase nuclei is unknown. Our *C. elegans* results suggest that two epitopes of Ce-titin each localize near the nuclear envelope. The anti-EU102 and anti-EU143 antibodies are unlikely to cross-react with lamins or other nuclear envelope proteins: (a) they were raised against different regions of the predicted Ce-titin polypeptide, (b) they do not recognize recombinant Ce-lamin on western blots (M.S.Z. and K.L.W., unpublished observations), and (c) the localization of EU102 at late stages of mitosis differs significantly from that of Ce-lamin (see Lee et al., 2000). Interestingly, the anti-EU143 antibodies recognize only one polypeptide of ~2.2 MDa in immunoblots of whole worm extracts, whereas anti-EU102 recognizes a ~500 kDa band (K. Ma, D.B.F., G. Gutierrez-Cruz, M. Houser, J. Pohl, G.M.B. and K. Wang, unpublished observations), leading us to speculate that nuclei express two isoforms of Ce-titin, both of which differ in size from twitchin (754 kDa) (Benian et al., 1993) and UNC-89 (732 kDa) (Benian et al., 1996). Ce-kettin is 470 kDa (Hakeda et al., 2000), so the EU102 antibody might crossreact with Ce-kettin. EU102 and EU143 are unlikely to recognize twitchin and UNC-89 because, in muscle EU102 and EU143 label the I-band (see Fig. 6) (D.B.F. and G.M.B., unpublished observations), whereas antibodies against twitchin (Moerman et al., 1988) and UNC-89 (Benian et al., 1996b; Small et al., 2004) localize to the outer and inner parts of the A-band, respectively. Our working hypothesis is that the EU102 epitope is present in a smaller (~500 kDa) nuclear isoform of Ce-titin. Clearly, much work remains to understand the splicing patterns and subnuclear localizations of Ce-titin.

The splicing and localizations of nuclear titin will also be interesting to pursue in human cells, because the C-terminal titin epitope recognized by serum 5460 did not concentrate at the nuclear envelope in HeLa cells. Instead, it localized diffusely throughout the nucleus, consistent with the localization of internal lamins, and in lamin-associated puncta. We are intrigued by the titin puncta, but further work is needed to determine what they represent (architectural 'nodes'?).

Why might titin bind lamins?

D-titin has essential roles during mitotic chromosome condensation (Machado and Andrew, 2000). Thus, in evolutionary terms, titin may have essential nuclear roles that predate the existence of muscle cells. However, the extent and nature of titin's nuclear roles are unknown. Our results show that Ce-titin localizes at least in part at the nuclear envelope, and depends on lamins for its localization during interphase. We do not know whether Ce-lamin depends on Ce-titin. We speculate that titin might link the lamina network to chromatin or nuclear actin, or both during interphase. Attempts to test these possibilities by downregulating Ce-titin expression in *C. elegans* have not yet succeeded (D.B.F, and G.M.B., unpublished observations). Nevertheless, our present findings emphasize an important point about nuclear structure: phenotypes seen in lamin-depleted or lamin-disrupted cells reflect the combined loss of lamins and all other structural proteins – now including titin – that depend on lamins.

Our limited current evidence suggests that, Ce-titin is either released from Ce-lamin or the Ce-titin epitope becomes masked relatively early in mitosis (metaphase), several minutes before Ce-lamin fully depolymerizes (in mid-late anaphase) (Lee et al., 2000). We speculate that the regulated detachment of titin from lamins helps to coordinate chromosome condensation and nuclear disassembly. Lamin filaments depolymerize gradually during mitosis (Moir et al., 2000b; Newport and Spann, 1987). This gradual shrinkage of the lamina network, still attached to chromosomes, might help to 'capture' condensing chromosomes within the mitotic spindle (Moir et al., 2000b). Given that D-titin is essential for chromosome condensation during mitosis, it will be interesting in future to test the hypothesis that two structural goliaths – titin filaments and lamin polymers – cooperatively orchestrate nuclear architecture during interphase, in addition to orchestrating large-scale events during mitosis.

Materials and Methods

Two-hybrid constructs and two-hybrid screening

The cDNA corresponding to *LMNA* exons 8-9, encoding residues 461-536, was PCR-amplified from a wild-type pre-lamin A cDNA using Taq polymerase (Invitrogen Inc, Carlsbad CA) and 5′ (5′-GAATTCGACCAGTCCATGGGCAATT-GG-3′) and 3′ (5′-GGATCCTTCCCGAGTGGAGTTGAT-3′) primers containing an *Eco*RI and *Bam*HI restriction site, respectively. After digestion with *Eco*RI and *Bam*HI (New England Biolabs, Beverly MA), the fragment was ligated into yeast two-hybrid bait vector pAS2.1 (ClonTech Inc., Palo Alto CA) using T4 DNA ligase (Invitrogen).

Each bait construct was transformed into yeast *MATa* strain AH109, and mated to yeast *MATα* strain Y187 pretransformed with a human skeletal muscle cDNA prey library (Matchmaker system, Clontech). Diploids with productive two-hybrid interactions were selected permissively on medium lacking amino acids Trp, Leu

and His (triple selection). Colonies that grew under triple selection were patched to plates that also lacked Ade (quadruple selection). Colonies that survived quadruple selection were assayed on filters for β-galactosidase activity per manufacturer instructions. Library plasmids isolated from each positive diploid colony were transformed into *E. coli* strain DH5α, purified, introduced into untransfected yeast strain Y187 and tested for autoactivation (growth on medium lacking Leu and His), or for β-galactosidase activity in the absence of the bait plasmid. Actin-encoding plasmids were identified in PCR reactions using actin-specific 5′ (5-GAG-GGCTACGCGCTGCCG-3′) and 3′ (5′-GCGCTCCGGGGCGATG-3′) primers.

Site-directed mutagenesis

Wild-type full length pre-lamin A in plasmid pET7a was a gift from Robert Goldman (Northwestern University, Chicago IL). Full length pre-lamin A carrying the L530P point-mutation was provided by Brian Burke (Univ. Florida, Gainesville, FL). Other missense mutations were introduced into pre-lamin A (QuickChange site-directed mutagenesis kit; Stratagene Inc, La Jolla CA) and confirmed by double stranded DNA sequencing (data not shown). Primers used to create each mutation were: R453W (5′ primer 5′-GGGCAAGTTTGTCTGGCTGCGCAACAAGTCC-3′ and 3′ primer 5′-GGACTTGTTGCGCAGCCAGACAAACTTGCCC-3′), R482Q (5′ primer 5′-CCCTTGCTGACTTACCAGTTCCCACC-3′ and 3′ primer 5′-GGTGGGAACTGGTAAGTCAGCAAGGG-3′), and R527P (5′ primer 5′-GCG-GGAACAGCCTGCCTACGGCTCTCATC-3′, and 3′ primer 5′-GATGAGAGC-CGTAGGCAGGCTGTTCCCGC-3′). The progeria lamin A construct was a gift from Hal Dietz and Dan Justice (Johns Hopkins School of Medicine) who generated a cDNA encoding the 50-residue deletion construct from patient cell cDNA.

Lamin tail constructs

Expression constructs for wild-type and mutated tail domains of human pre-lamin A, and mature lamin B1 were made by PCR amplification with the primers listed below, using either wild-type or mutated cDNAs as templates, and then shuttled into plasmid pET23b (Novagen). The 5′ and 3′ primers used for pre-lamin A tail residues 394-664 were 5′-GGATCCTACCTCGCAGCGCSGCCGTGGCCG-3′ and 5′-CTCGCGTTACATGATGCTGCAGTTCTGGGG-3′, respectively; for lamin B1 tail residues 395-586 the primers were 5′-GGATCCTTCTTCCCGTGTGACAC-TATCCC-3′ and 5′-CTCGAGTTACATAATTGCACAGCTTC3′, respectively.

Ni^{2+}-agarose pull-down assays

Purified His-tagged recombinant lamin tail proteins were desalted using Quick Spin Protein Columns (Roche) to remove excess imidazole and equilibrated in PBS with 10 mM imidazole (PBSI). We then incubated 300 μg lamin tail proteins (A, B1, or mutants) 1 hour at 22-24°C with 500 ul Ni^{2+} NTA-agarose-bead slurry (Qiagen), with gentle rotation. Beads were then washed three times in PBSI (1 ml each) and resuspended (final volume, 1 ml) in PBSI. Aliquots (100 μl) of bead slurry were then added to tubes containing 80 μl PBSI plus 20 μl ^{35}S-titin produced in eukaryotic transcription and translation reactions (described below), and incubated 1 hour at 22-24°C with gentle rotation. Beads were washed five times in PBSI (1 ml each), final pellets were resuspended in 50 μl 2×SDS-sample buffer, and samples were resolved by SDS-PAGE (12% acrylamide), dried and exposed to film for two days.

Expression of titin 1-551 subfragments and synthesis of ^{35}S-probes

Ig-fold domains in titin 1-551 were identified using the SWISS-MODEL program (www.expasy.org). The primers used to PCR-amplify sub-fragments 1-6 of titin 1-551 were designed specifically for use in coupled transcription and translation reactions: each 5′ primer included a T7 promoter (TAATACGACTCACTATAGGG) 5′ of the titin ORF to enhance translation initiation, and each 3′ primer included a stop codon followed by poly-dTTP (dT_{30}) to terminate translation. The resulting PCR products were synthesized in coupled eukaryotic transcription/translation reactions (TNT kit, Promega Corp., Madison WI) in the presence of ^{35}S-Met-Cys (ProMix; Amersham), per manufacturer instructions. Each TNT reaction was passed over a Quick Spin Protein Column (Roche) to remove unincorporated counts.

Microtiter-well binding assays

Microtiter assays were done as described (Holaska et al., 2003). In brief, purified lamin A tail proteins were allowed to adhere to microtiter wells in solution, blocked with BSA and then incubated with increasing concentrations of ^{35}S-titin 1-551. Plates were washed, bound proteins were eluted with 5% SDS, and signals were quantified using a scintillation counter. All assays were done in triplicate.

Western blot analysis with 5460 serum

Protein lysates of whole HeLa cells transfected with GFP-is6 were resolved by SDS-PAGE, transferred to nitrocellulose, blocked with 5% milk in PBS and probed at dilutions of 1:10,000 with either immune serum 5460 (bleed 3), immune serum 5460 pre-incubated with purified antigen (M-is6 polypeptide), or pre-immune serum 5460. For analysis of large endogenous titin proteins, HeLa cells or isolated HeLa cell nuclei (see below) were lysed as described (Machado et al., 1998), and immediately resolved by 2.5-7.5% gradient SDS-PAGE, transferred to nitrocellulose and blocked as described (Machado et al., 1998), then probed with serum 5460 at the dilution of 1:10,000.

Staining of untransfected HeLa cells and isolated nuclei

HeLa cell nuclei were isolated as described (Dean and Kasamatsu, 1994). Isolated nuclei were adhered to poly-L-lysine-coated coverslips. Nuclei and whole HeLa cells were fixed 15 minutes in 3.7% formaldehyde, permeabilized 20 minutes in PBS with 0.1% Triton X-100, blocked in PBS with 3% BSA and incubated 2 hours with rabbit serum 5460 [with or without preincubation with 1:1 (v/v) purified M-is6 antigen at 1 mg/ml] at 1:1000 dilution in PBS with 3% BSA. Mouse monoclonal antibody NCL-LAM-A/C (Novacastra, Newcastle, UK) against A-type lamins was used at 1:250 dilution. Cy3-labeled goat anti-rabbit and FITC-labeled goat anti-mouse secondary antibodies (Jackson ImmunoResearch) were used at 1:1000 dilution. Cells were imaged as described below for HeLa cells.

GFP fusions and transient expression in HeLa cells

To generate GFP-fusion proteins, we first PCR amplified the titin M-is6 and M-is7 polypeptides using 5′ primers containing a *Bgl*II site and an encoded nuclear localization signal (NLS; PPKKKRKV), and 3′ primers containing a *Bam*HI site. Products from PCR reactions were ligated into pGEMT (Promega) per manufacturer protocol. Inserts were removed from pGEMT by digestion with *Bam*HI and *Bgl*II, ligated (DNA Rapid Ligation kit; Roche) into the peGFP-C1 vector (Clontech), digested with *Bam*HI and *Bgl*II then treated with 2 units of calf intestine phosphatase for 1 hour at 37°C (Gibco BRL). M-is6 and M-is7 were then each ligated into peGFP-C1 using T4 DNA ligase (New England Biolabs, Beverly, MA). The GFP-PK construct was provided by Diane Hayward (Johns Hopkins School of Medicine, Baltimore, MD) (Chen et al., 2001). Each construct was transfected into HeLa cells using LT1 transfection reagent (Mirus; Madison, WI). After 24 hours, cells were fixed in 3.7% formaldehyde for 15 minutes, permeabilized 20 minutes in PBS with 0.2% Triton X-100, then blocked in PBS with 3% BSA for 1 hour and incubated 2 hours each in primary and secondary antibody. Rabbit polyclonal serum specific for lamin B (NC-9 antibody, generous gift from Nilabh Chaudhary (Ridgeway Biosystems Inc., Cleveland, OH) was used at 1:1000 dilution. Goat anti-rabbit Cy3-conjugated secondary antibody (Jackson ImmunoResearch) was used at 1:1000 dilution. HeLa cells were imaged using a Nikon Eclipse E600 equipped with a Nikon Plan Fluo 40X N.A. 0.75 dry objective. Images were acquired with a Q Imagine Retiga Exi 12 bit digital camera using IPLab version 3.9.3r4 software from Scanalytics, Inc.

Immunoprecipitation of transfected HeLa cells

Confluent 10-cm plates of HeLa cells were pelleted 24 hours after transfection with cDNAs encoding GFP fusions, resuspended in 1 ml lamin solubilization buffer (10 mM Tris, pH 7.4, 1 mM EDTA, 1% NP40, 1% Triton X-100, 1% SDS, 1 M NaCl) and diluted with nine volumes of 10 mM Tris pH 7.4, 1 mM EDTA. This diluted cell lysate (200 μl) was then incubated with 10 μl mouse monoclonal anti-GFP (Santa Cruz Biotechnology Inc., Santa Cruz, CA) for 30 minutes at 22-24°C. Protein A magnetic beads (50 μl; New England Biolabs, Beverly, MA) were added and rotated 1 hour at 22-24°C, then washed and isolated according to the manufacturer's instructions, but using 276 mM NaCl, 2.5 mM KCl, 1.5 mM KH_2PO_4, 0.1% Triton X-100 as the wash buffer. Ten percent of each pellet and supernatant were resolved on 12% SDS-PAGE gels transferred to Protran nitrocellulose (Schleicher and Schuell Bioscience, Dassel, Germany) and probed with a mixture of two antibodies: rabbit serum NC-5 (against A-type lamins) and rabbit serum NC-9 (against lamin B1), both gifts from N. Chaudhary.

C. elegans strains and culture

C. elegans wild-type strain Bristol (N2) was cultured as described (Brenner, 1974).

Antisera production

Rabbit serum 5460 was generated against the bacterially expressed, purified and untagged human titin M-is6 polypeptide (residues 62-172 of the 1-551 fragment; Covance Research Products, Denver, PA), and used at dilutions of 1:1000 for immunofluorescence and 1:10,000 for immunoblotting.

Ce-titin polyclonal serum EU102 has been described previously (Flaherty et al., 2002). Guinea pig serum EU145 was raised against the N-terminal 314 residues of the predicted 2.2 MDa isoform of Ce-titin, and rat serum EU143 was raised against the predicted C-terminal 353 residues. Both antigens were expressed as GST fusion proteins in *E. coli*. cDNAs encoding antigenic polypeptides were amplified by RT-PCR using Pfu polymerase (Stratagene) and primers containing added *Xho*I and *Eco*RI sites. The 5′ and 3′ primers for EU145 were 5′-GTACGAATTCAT-GGAGGGCAACGAGAAGAAAGG-3′ and 5′-GATGCTCGAGCATTGGGTC-AAAGGCAGTGGTCG-3′, respectively. The primers for EU143 were 5′-GTA-CGAATTCAAATTCATCTCAGTGACACCAGG-3′ and 5′-GATGCTCGAGCTA-CCGACGAATCGTTCTTCGTTG-3′, respectively. Each amplified product was cloned into pGEX-6P-1 (Amersham Pharmacia Biotech). The GST fusion proteins were expressed and purified as described (Flaherty et al., 2002). Milligram quantities of fusion proteins were supplied to Spring Valley Laboratories

(Sykesville, MD) for antiserum production. Both EU145 and EU143 were affinity purified as described (Benian et al., 1993).

C. elegans muscle immunofluorescence microscopy

Adult nematodes were stained by indirect immunofluorescene as described (Benian et al., 1996b). Fluorescent images were acquired with a scientific-grade, cooled charge-coupled device (Cool-Snap HQ with ORCA-ER chip) on a multi-wavelength widefield 3D microscopy system (Intelligent Imaging Innovations) based on a Zeiss Axiovert 200M inverted microscope equipped with a 63×/1.4-NA objective. Images were collected at 22-24°C using a standard Sedat filter set (Chroma) in successive 0.20 μm focal planes through each sample, and out-of-focus light was removed with a 23 constrained iterative deconvolution algorithm (Swedlow et al., 1997).

RNAi downregulation of *lmn-1* and indirect immunofluorescence of *C. elegans* embryos

The *C. elegans* lamin gene (*lmn-1*) was downregulated by the feeding method as described (Gruenbaum et al., 2002). Control worms were grown on *E. coli* strain OP50.

To stain by indirect immunofluorescence, 12 wild-type or RNAi-treated larva or adult *C. elegans* were placed into 10 μl PBT [PBS containing 0.1% *(w/v) BSA and 0.1% Triton X-100] on poly-lysine-treated slides. A 45-mm coverslip was then placed over the slide and tapped gently until embryos were extruded from the adult vulva. Microscope slides were then frozen by placing onto dry ice, coverslips were popped off and worms fixed immediately in methanol at –20°C (20 minutes) followed by acetone (–20°C, 20 minutes). Slides were then washed three times (15 minutes each) with PBT to block nonspecific epitopes. Affinity-purified antibodies against Ce-titin were used at dilutions of 1:200 (EU102), 1:50 (EU143) or 1:100 (EU145). Serum 3932 (rabbit) or 3933 (rat) antibodies against Ce-lamin were used at 1:500 dilution (Gruenbaum et al., 2002). Primary antibodies were incubated overnight at 4°C with gentle rocking. Slides were washed three times (15 minutes each) in PBT, then incubated 3 hours at 22°C in a final volume of 50 μl secondary antibody (diluted 1:1000; Jackson Immuno Research, Inc). Samples were washed three times (15 minutes each) in PBT, incubated 5 minutes in PBT containing 1 μg/ml DAPI to stain DNA, and washed once (5 minutes) in 8 ml PBT. Fluorescence was protected with 8 μl Vectashield (Vector Laboratories, Inc.), prior to adding a coverslip (size 1; Fisher Scientific) and sealing. Slides were imaged using a Zeiss Axiovert 200 microscope equipped with an Ultraview confocal imaging system (Perkin Elmer) using a 40× NA 1.3 Zeiss Plan-FLUAR oil objective at room temperature. Images were acquired as single 1 μM optical sections and color-merged using Perkin Elmer Imaging Suite software (version 5.5). Contrast was adjusted and figures were assembled using Adobe Photoshop software (version 7.0) and CorelDRAW 10.

We thank D. Andrew, A. Forer, Y. Gruenbaum, J. Holaska, K. Lee, K. Tifft, and R. Montes de Oca for enlightening conversation and comments on the manuscript. We thank R. Goldman, N. Chaudhary, D. Hayward, B. Burke, M. Powers, H. Dietz and D. Justice for constructs and reagents. We gratefully acknowledge C. DeRenzo and G. Seydoux for help with *C. elegans*, and the Johns Hopkins Microscope Facility for help with imaging. We also thank D. Kalman for use of his deconvolution microscopy system. M.S.Z. thanks Lois Zastrow for inspiration. This work was funded by grants from NIH (AR51466-01 to G.M.B. and GM64535, to K.L.W.) and the Ray Mills Fund (to K.L.W.).

References

Aebi, U., Cohn, J., Buhle, L. and Gerace, L. (1986). The nuclear lamina is a meshwork of intermediate-type filaments. *Nature* **323**, 560-564.

Amodeo, P., Fraternali, F., Lesk, A. M. and Pastore, A. (2001). Modularity and homology: modelling of the titin type I modules and their interfaces. *J. Mol. Biol.* **311**, 283-296.

Benian, G. M., L'Hernault, S. W. and Morris, M. E. (1993). Additional sequence complexity in the muscle gene, unc-22, and its encoded protein, twitchin, of Caenorhabditis elegans. *Genetics* **134**, 1097-1104.

Benian, G. M., Tang, X. and Tinley, T. L. (1996a). Twitchin and related giant Ig superfamily members of C. elegans and other invertebrates. *Adv. Biophys.* **33**, 183-198.

Benian, G. M., Tinley, T. L., Tang, X. and Borodovsky, M. (1996b). The Caenorhabditis elegans gene unc-89, required for muscle M-line assembly, encodes a giant modular protein composed of Ig and signal transduction domains. *J. Cell Biol.* **132**, 835-848.

Bonne, G., Di Barletta, M. R., Varnous, S., Becane, H. M., Hammouda, E. H., Merlini, L., Muntoni, F., Greenberg, C. R., Gary, F., Urtizberea, J. A. et al. (1999). Mutations in the gene encoding lamin A/C cause autosomal dominant Emery-Dreifuss muscular dystrophy. *Nat. Genet.* **21**, 285-288.

Brenner, S. (1974). The genetics of Caenorhabditis elegans. *Genetics* **77**, 71-94.

Chen, L., Liao, G., Fujimuro, M., Semmes, O. J. and Hayward, S. D. (2001). Properties of two EBV Mta nuclear export signal sequences. *Virology* **288**, 119-128.

Chen, L., Lee, L., Kudlow, B. A., Dos Santos, H. G., Sletvold, O., Shafeghati, Y., Botha, E. G., Garg, A., Hanson, N. B., Martin, G. M. et al. (2003). LMNA mutations in atypical Werner's syndrome. *Lancet* **362**, 440-445.

Cohen, M., Lee, K. K., Wilson, K. L. and Gruenbaum, Y. (2001). Transcriptional repression, apoptosis, human disease and the functional evolution of the nuclear lamina. *Trends Biochem. Sci.* **26**, 41-47.

Dahl, K. N., Kahn, S. M., Wilson, K. L. and Discher, D. E. (2004). The nuclear envelope lamina network has elasticity and a compressibility limit suggestive of a molecular shock absorber. *J. Cell Sci.* **117**, 4779-4786.

De Sandre-Giovannoli, A., Chaouch, M., Kozlov, S., Vallat, J., Tazir, M., Kassouri, N., Szepetowski, P., Hammadouche, T. V. A., Stewart, C. L., Grid, D. et al. (2002). Homozygous defects in LMNA, encoding lamin A/C nuclear-envelope proteins, cause autosomal recessive axonal neuropathy in human (Charcot-Marie-Tooth Disorder Type 2) and mouse. *Am. J. Hum. Genet.* **70**, 726-736.

De Sandre-Giovannoli, A., Bernard, R., Cau, P., Navarro, C., Amiel, J., Boccaccio, I., Lyonnet, S., Stewart, C. L., Munnich, A., Le Merrer, M. et al. (2003). Lamin A Truncation in Hutchinson-Gilford Progeria. *Science* **300**, 2055.

Dean, D. A. and Kasamatsu, H. (1994). Signal- and energy-dependent nuclear transport of SV40 Vp3 by isolated nuclei. Establishment of a filtration assay for nuclear protein import. *J. Biol. Chem.* **269**, 4910-4916.

Dhe-Paganon, S., Werner, E. D., Chi, Y. I. and Shoelson, S. E. (2002). Structure of the globular tail of nuclear lamin. *J. Biol. Chem.* **277**, 17381-17384.

Eriksson, M., Brown, W. T., Gordon, L. B., Glynn, M. W., Singer, J., Scott, L., Erdos, M. R., Robbins, C. M., Moses, T. Y., Berglund, P. et al. (2003). Recurrent de novo point mutations in lamin A cause Hutchinson-Gilford progeria syndrome. *Nature* **423**, 293-298.

Flaherty, D. B., Gernert, K. M., Shmeleva, N., Tang, X., Mercer, K. B., Borodovsky, M. and Benian, G. M. (2002). Titins in C.elegans with unusual features: coiled-coil domains, novel regulation of kinase activity and two new possible elastic regions. *J. Mol. Biol.* **323**, 533-549.

Fridkin, A., Mills, E., Margalit, A., Neufeld, E., Lee, K. K., Feinstein, N., Cohen, M., Wilson, K. L. and Gruenbaum, Y. (2004). Matefin, a Caenorhabditis elegans germ line-specific SUN-domain nuclear membrane protein, is essential for early embryonic and germ cell development. *Proc. Natl. Acad. Sci. USA* **101**, 6987-6992.

Goldman, R. D., Gruenbaum, Y., Moir, R. D., Shumaker, D. K. and Spann, T. P. (2002). Nuclear lamins: building blocks of nuclear architecture. *Genes Dev.* **16**, 533-547.

Granzier, H. L. and Labeit, S. (2004). The giant protein titin: a major player in myocardial mechanics, signaling, and disease. *Circ. Res.* **94**, 284-295.

Gruenbaum, Y., Lee, K. K., Liu, J., Cohen, M. and Wilson, K. L. (2002). The expression, lamin-dependent localization and RNAi depletion phenotype for emerin in *C. elegans*. *J. Cell Sci.* **115**, 923-929.

Gruenbaum, Y., Goldman, R. D., Meyuhas, R., Mills, E., Margalit, A., Fridkin, A., Dayani, Y., Prokocimer, M. and Enosh, A. (2003). The nuclear lamina and its functions in the nucleus. *Int. Rev. Cytol.* **226**, 1-62.

Gruenbaum, Y., Margalit, A., Goldman, R. D., Shumaker, D. K. and Wilson, K. L. (2005). The nuclear lamina comes of age. *Nat. Rev. Mol. Cell. Biol.* **6**, 21-31.

Hackman, J. P., Vihola, A. K. and Udd, A. B. (2003). The role of titin in muscular disorders. *Ann. Med.* **35**, 434-441.

Hakeda, S., Endo, S. and Saigo, K. (2000). Requirements of Kettin, a giant muscle protein highly conserved in overall structure in evolution, for normal muscle function, viability, and flight activity of Drosophila. *J. Cell Biol.* **148**, 101-114.

Harborth, E. S., Elbashir, S. M., Bechert, K., Tuschl, T. and Weber, K. (2001). Identification of essential genes in cultured mammalian cells using small interfering RNAs. *J. Cell Sci.* **114**, 4557-4565.

Holaska, J. M., Lee, K. K., Kowalski, A. K. and Wilson, K. L. (2003). Transcriptional repressor germ cell-less (GCL) and barrier-to-autointegration factor (BAF) compete for binding to emerin in vitro. *J. Biol. Chem.* **278**, 6969-6975.

Izumi, M., Vaughan, O. A., Hutchinson, C. J. and Gilbert, D. M. (2000). Head and/or CaaX domain deletions of lamin proteins disrupt preformed lamin A and C but not lamin B structure in mammalian cells. *Mol. Biol. Cell* **11**, 4323-4337.

Krimm, I., Ostlund, C., Gilquin, B., Couprie, J., Hossenlopp, P., Mornon, J. P., Bonne, G., Courvalin, J. C., Worman, H. J. and Zinn-Justin, S. (2002). The Ig-like structure of the C-terminal domain of lamin A/C, mutated in muscular dystrophies, cardiomyopathy, and partial lipodystrophy. *Structure (Camb.)* **10**, 811-823.

Labeit, S. and Kolmerer, B. (1995). Titins: giant proteins in charge of muscle ultrastructure and elasticity. *Science* **270**, 293-296.

Lammerding, J., Schulze, P., Takahashi, T., Kozlov, S., Sullivan, T., Kamm, R., Stewart, C. and Lee, R. (2004). Lamin A/C deficiency causes defective nuclear mechanics and mechanotransduction. *J. Clin. Invest.* **113**, 370-378.

Lange, S., Xiang, F., Yakovenko, A., Vihola, A., Hackman, P., Rostkova, E., Kristensen, J., Brandmeier, B., Franzen, G., Hedberg, B. et al. (2005). The kinase domain of titin controls muscle gene expression and protein turnover. *Science* **308**, 1599-1603.

Lee, K. K., Gruenbaum, Y., Spann, P., Liu, J. and Wilson, K. L. (2000). C. elegans nuclear envelope proteins emerin, MAN1, lamin, and nucleoporins reveal unique timing of nuclear envelope breakdown during mitosis. *Mol. Biol. Cell* **11**, 3089-3099.

Lin, F. and Worman, H. J. (1993). Structural organization of the human gene encoding nuclear lamin A and nuclear lamin C. *J. Biol. Chem.* **268**, 16321-16326.

Lin, F. and Worman, H. J. (1995). Structural organization of the human gene (LMNB1) encoding nuclear lamin B1. *Genomics* **27**, 230-236.

Linke, W. A., Kulke, M., Li, H., Fujita-Becker, S., Neagoe, C., Manstein, D. J., Gautel,

M. and Fernandez, J. M. (2002). PEVK domain of titin: an entropic spring with actin-binding properties. *J. Struct. Biol.* **137**, 194-205.
Liu, J., Ben-Shahar, T. R., Riemer, D., Treinin, M., Spann, P., Weber, K., Fire, A. and Gruenbaum, Y. (2000). Essential roles for Caenorhabditis elegans lamin gene in nuclear organization, cell cycle progression, and spatial organization of nuclear pore complexes. *Mol. Biol. Cell* **11**, 3937-3947.
Liu, J., Lee, K. K., Segura-Totten, M., Neufeld, E., Wilson, K. L. and Gruenbaum, Y. (2003). MAN1 and emerin have overlapping function(s) essential for chromosome segregation and cell division in Caenorhabditis elegans. *Proc. Natl. Acad. Sci. USA* **100**, 4598-4603.
Machado, C. and Andrew, D. J. (2000). D-Titin: a giant protein with dual roles in chromosomes and muscles. *J. Cell Biol.* **151**, 639-652.
Machado, C., Sunkel, C. E. and Andrew, D. J. (1998). Human autoantibodies reveal titin as a chromosomal protein. *J. Cell Biol.* **141**, 321-333.
Mancini, M. A., Shan, B., Nickerson, J. A., Penman, S. and Lee, W. H. (1994). The retinoblastoma gene product is a cell cycle-dependent, nuclear matrix-associated protein. *Proc. Natl. Acad. Sci. USA* **91**, 418-422.
Mislow, J. M. K., Holaska, J. M., Kim, M. S., Lee, K. K., Segura-Totten, M., Wilson, K. L. and McNally, E. M. (2002a). Nesprin-1α self-associates and binds directly to emerin and lamin A in vitro. *FEBS Lett.* **525**, 135-140.
Mislow, J. M. K., Kim, M. S., Davis, D. B. and McNally, E. M. (2002b). Myne-1, a spectrin repeat transmembrane protein of the myocyte inner nuclear membrane, interacts with lamin A/C. *J. Cell Sci.* **115**, 61-70.
Moerman, D. G., Benian, G. M., Barstead, R. J., Schreifer, L. and Waterston, R. H. (1988). Identification and intracellular localization of the unc-22 gene product of *C. elegans*. *Genes Dev*. **2**, 93-105.
Moir, R. D., Yoon, M., Khuon, S. and Goldman, R. D. (2000a). Nuclear lamins A and B1: different pathways of assembly during nuclear envelope formation in living cells. *J. Cell Biol.* **151**, 1155-1168.
Moir, R. D., Spann, T. P., Lopez-Soler, R. I., Yoon, M., Goldman, A. E., Khuon, S. and Goldman, R. D. (2000b). The dynamics of the nuclear lamins during the cell cycle – relationship between Structure and Function. *J. Struct. Biol.* **129**, 324-334.
Mounkes, L. C. and Stewart, C. L. (2004). Aging and nuclear organization: lamins and progeria. *Curr. Opin. Cell Biol.* **16**, 322-327.
Navarro, C. L., De Sandre-Giovannoli, A., Bernard, R., Boccaccio, I., Boyer, A., Genevieve, D., Hadj-Rabia, S., Gaudy-Marqueste, C., Smitt, H. S., Vabres, P. et al. (2004). Lamin A and ZMPSTE24 (FACE-1) defects cause nuclear disorganization and identify restrictive dermopathy as a lethal neonatal laminopathy. *Hum. Mol. Genet.* **13**, 2493-2503.
Newport, J. and Spann, T. (1987). Disassembly of the nucleus in mitotic extracts: membrane vesicularization, lamin disassembly, and chromosome condensation are independent processes. *Cell* **48**, 219-230.
Novelli, G., Muchir, A., Sangiuolo, F., Helbing-Leclerc, A., D'Apice, M. R., Massart, C., Capon, F., Sbraccia, P., Federici, M., Lauro, R. et al. (2002). Mandibuloacral dysplasia is caused by a mutation in *LMNA*-encoding lamin A/C. *Am. J. Hum. Genet.* **71**, 426-431.
Ostlund, C. and Worman, H. J. (2003). Nuclear envelope proteins and neuromuscular diseases. *Muscle Nerve* **27**, 393-406.
Padmakumar, V. C., Abraham, S., Braune, S., Noegel, A. A., Tunggal, B., Karakesisoglou, I. and Korenbaum, E. (2004). Enaptin, a giant actin-binding protein, is an element of the nuclear membrane and the actin cytoskeleton. *Exp. Cell Res.* **295**, 330-339.
Pederson, T. and Aebi, U. (2002). Actin in the nucleus: what form and what for? *J. Struct. Biol.* **140**, 3-9.
Sasseville, A. M. and Langelier, Y. (1998). In vitro interaction of the carboxy-terminal domain of lamin A with actin. *FEBS Lett.* **425**, 485-489.
Shackleton, S., Lloyd, D. J., Jackson, S. N., Evans, R., Niermeijer, M. F., Singh, B. M., Schmidt, H., Brabant, G., Kumar, S., Durrington, P. N. et al. (2000). LMNA, encoding lamin A/C, is mutated in partial lipodystrophy. *Nat. Genet.* **24**, 153-156.
Small, T. M., Gernert, K. M., Flaherty, D. B., Mercer, K. B., Borodovsky, M. and Benian, G. M. (2004). Three new isoforms of Caenorhabditis elegans UNC-89 containing MLCK-like protein kinase domains. *J. Mol. Biol.* **342**, 91-108.
Spann, T. P., Goldman, A. E., Wang, C., Huang, S. and Goldman, R. D. (2002). Alteration of nuclear lamin organization inhibits RNA polymerase II-dependent transcription. *J. Cell Biol.* **156**, 603-608.
Steen, R. L. and Collas, P. (2001). Mistargeting of B-type lamins at the end of mitosis: implications on cell survival and regulation of lamins A/C expression. *J. Cell Biol.* **153**, 621-626.
Stuurman, N., Heins, S. and Aebi, U. (1998). Nuclear lamins: their structure, assembly, and interactions. *J. Struct. Biol.* **122**, 42-66.
Sullivan, T., Escalente-Alcalde, D., Bhatt, H., Anver, M., Naryan, B., Nagashima, K., Stewart, C. L. and Burke, B. (1999). Loss of A-type lamin expression compromises nuclear envelope integrity leading to muscular dystrophy. *J. Cell Biol.* **147**, 913-920.
Swedlow, J. R., Sedat, J. W. and Agard, D. A. (1997). Deconvolution in optical microscopy. In *Deconvolution of images and spectra* (ed. P. A. Jansson), pp. 284-307. San Diego: Academic Press.
Tskhovrebova, L. and Trinick, J. (2003). Titin: properties and family relationships. *Nat. Rev. Mol. Cell. Biol.* **4**, 679-689.
Zastrow, M. S., Vlcek, S. and Wilson, K. L. (2004). Proteins that bind A-type lamins: integrating isolated clues. *J. Cell Sci.* **117**, 979-987.
Zhang, Q., Skepper, J. N., Yang, F., Davies, J. D., Hegyi, L., Roberts, R. G., Weissberg, P. L., Ellis, J. A. and Shanahan, C. M. (2001). Nesprins: a novel family of spectrin-repeat-containing proteins that localize to the nuclear membrane in multiple tissues. *J. Cell Sci.* **114**. 4485-4498.
Zhang, Q., Ragnauth, C., Greener, M. J., Shanahan, C. M. and Roberts, R. G. (2002). The nesprins are giant actin-binding proteins, orthologous to Drosophila melanogaster muscle protein MSP-300. *Genomics* **80**, 473-481.

Journal of Cell Science